Liquid-Liquid Extraction of Aroma Compounds with Hollow Fiber Contactor

Arnaud Baudot, Juliane Floury and Herbert E. Smorenburg
Unilever Research Vlaardingen, 3130 AC Vlaardingen, The Netherlands

The extraction of aroma compounds through a commercial hollow-fiber contactor from model aqueous feeds to sunflower oil was tested. The stripping efficiency of this membrane-based solvent extraction operation was systematically studied as a function of the oil/water partition coefficient of the permeants, and the flow and location of the feeds in the contactor (in the shell side or in the lumen of the fibers). The mass transfer between the two phases was modeled based on the resistances-in-series approach. In particular, a correlation describing the mass transfer with a transverse flow in the shell is proposed. With similar operating conditions, the stripping of the aroma compounds was more efficient when flowing the aqueous feed phase in the shell side than inside the fibers.

Introduction

Nowadays, aroma concentrates are widely used in the food industry to improve the flavor of formulated foods or to compensate for the flavor losses of natural raw products during industrial processing. Consumers are more attracted to food products containing only "natural" or "nature-identical" additives, either for health reasons (as synthetic compounds are likely to contain traces of harmful organic reactants), or simply because they provide a richer and more subtle sensory profile. Those "natural"-labeled aroma compounds are generally found at very low concentration (in the PPM range) in natural raw materials or in biosynthesis fermentation broths. Therefore, a cost-effective and efficient extraction step constitutes a major challenge for the production of such additives by the flavor industry. In order to recover odor-active organic substances from aqueous streams, the flavor industry relies mainly on the two main specific physico-chemical properties of flavor compounds:

Volatility: The distillation process has been the war-horse of the flavor industry for centuries. This method is efficient mainly for the "lighter" compounds, which generally display a low boiling temperature at atmospheric pressure. However, this method is extremely energy-costing (due to the phase change of the feed) and heat-sensitive compounds can easily get spoiled with such a treatment. Moreover, the vapor-liquid-phase change is generally not favorable for the recovery of high-boiling flavor compounds. An alternative way to the distillation is the pervaporation technique that associates the evaporation of the aroma compounds with a selective transport by sorption and diffusion of the organic compounds through a dense polymer layer. Although this novel technique generally leads to an enhancement of selectivity if compared to distillation, the solution-diffusion transport step through the membrane induces low transmembrane fluxes (Baudot and Marin, 1997) which, until now, has limited the adoption of this technique in the flavor industry.

Hydrophobicity: The best option to recover the "heavier" fraction of a flavor cocktail is the extraction with a medium for which the aroma compounds display a better affinity. As the high-boiling compounds often display a pronounced hydrophobic behavior, solvent extraction is the easiest way to recover these molecules from biological aqueous streams. The most common organic solvents used by flavor houses are ethanol, ether, small alkanes, acetone, and chlorinated hydrocarbons. Other extraction techniques have also been investigated, but they still constitute a minor part of the extraction operations carried out in the flavor industry. For instance, hydrophobic solid adsorbents have been recently applied with success for the sorption of aroma compounds (Souchon et al., 1996). Supercritical extraction also permits

Correspondence concerning this article should be addressed to H. E. Smorenburg.
Current address of A. Baudot: IFP-Département Techniques de Séparation (RG 40), 1 et 4 avenue de Bois-Préau, F-92852 Rueil-Malmaison, France.
Current address of J. Floury: GEPEA-ENITIAA, DGPA, Rue de la Géraudière, BP 82225, 44322 Nantes Cedex 3, France.

recovery of very high quality aroma extracts (Starmans and Nijhuis, 1996). However, the high capital and operating costs, as well as the batch nature of this technique, still limit its use in the production of compounds with a very high added value.

Conventional solvent extraction has been used in the chemical industry for over a century. The main challenge in designing and operating a solvent extraction operation is the maximization of the mass transfer by producing as much interfacial area as possible between the stripped feed and the solvent (which is generally immiscible with the stripped feed). This is achieved by dispersion in mixer-settlers devices or by a judicious selection of the packing material in columns. However, this conventional equipment has many disadvantages: the need of dispersion and coalescence, problems of emulsification, flooding and loading limits in continuous countercurrent devices, the need for a density difference between the phases, and the high maintenance costs of centrifugal apparatus.

In order to overcome all these drawbacks, an alternative approach consists of immobilizing the interface between the stripped feed and the solvent inside a porous membrane. Research on this so-called "membrane-based solvent extraction" technique (MSE) has been promoted mainly in the late 1980s by the respective teams of Sirkar (Prasad and Sirkar, 1987; Frank and Sirkar, 1985) and Cussler (Dahuron and Cussler, 1988; Yang and Cussler, 1986). Gabelman and Hwang (1999) have recently issued the most extensive literature review of the results published so far, on the MSE technique.

In the food area, few studies concerning the membrane-based solvent extraction of aroma compounds have been published. The first use of these membrane contactors for the solvent extraction of flavor compounds was reported by Souchon (1994). This author used a Liqui-Cel module (produced by the Celgard company) as a continuous extraction step coupled to a bioreactor in order to boost the yield of the biotransformation of methyl ricinoelate by *Sporidiobolus salmonicolor* strains into γ-decalactone, a valuable peach-like aroma compound. The flavor-containing fermentation broth flowed through the lumen of the hollow fibers while hexane, used as the stripping medium, flowed in the shell side. This lactone production technique was patented later (Spinnler et al., 1994). Another article also states the use of membrane-based solvent extraction with Liqui-Cel modules. This study was aimed at the concentration/recovery of phenylethyl alcohol, a rose-like fragrance mainly used in perfumery (Fabre et al., 1996). These two research works were mainly feasibility studies and demonstrated the advantages of MSE for the recovery of flavor compounds over conventional solvent extraction operations. However, the performances of this technique were not systematically screened as a function of the operating conditions and no general model was provided by these authors.

Aim of the Study. It was chosen to systematically study the performance of the membrane-based solvent extraction of aroma compounds from an aqueous feed with a commercial hollow fiber contactor.

The first part of the study consisted of an experimental investigation of the extraction of flavor compounds from water to sunflower oil (later on also named as *solvent*) over a very broad range of operating conditions. Attention was particularly focused on the effect of the following parameters on the stripping efficiency:

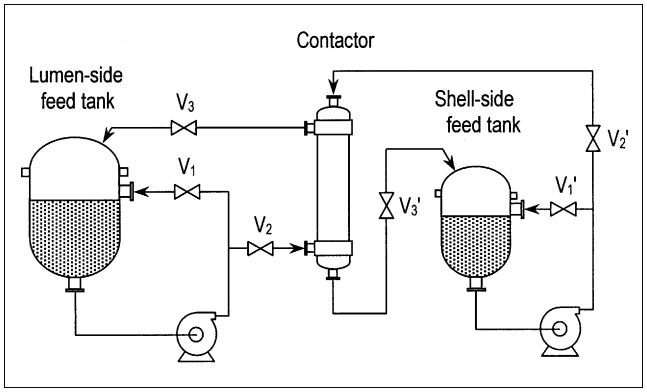

Figure 1. Set-up.

- Oil/water partition (distribution) coefficient of the stripped compounds (using eight aroma compounds with solvent/water partition coefficient ranging from 1 to 2,000).
- Effect of the flavored aqueous feed flow (ranging from 0.7 to 450 L/h)
- Respective location of the feeds (either in the lumen of the hollow-fibers or in the shell side).

In the second part of the study, a predictive model of the mass transfer between the two phases in the whole range of experimental operating conditions was proposed. In particular, because of the scarce number and the inhomogeneity of the models found in the literature, a new correlation was introduced to describe the mass transfer in the baffled shell of the studied contactor. It was also shown that MSE could prove to be a selective extraction technique for the most lipophilic compounds. Finally, the efficiency of the membrane-based solvent extraction technique was compared with more conventional extraction techniques and the potential applications of this technique in the food area were discussed.

Materials and Methods

The two phases were recirculated on each side of the membrane (Figure 1) until the equilibrium between the two phases was reached. The stripped feed phase was composed of distilled water in which the various aroma compounds to be extracted were dissolved. During the experiments, the aroma compounds were diffusing from the aqueous stripped feed through the membrane to the stripping phase (also referred to in the text as "solvent," or "stripping phase") which consisted of commercial sunflower oil. Sunflower oil was chosen as the solvent because: (1) it is not miscible with water; (2) it displays a hydrophobic behavior; and (3) it is edible. As a consequence, if the aroma extract was to be reused for food formulation, the flavored oil could be used directly as a flavoring additive, without further treatment.

The experiments were carried out with a recirculation of the fluids in the feed tanks ("off-line" or "batch" configuration) for practical convenience. Indeed, most of the results in the literature have been obtained with such a configuration. Nevertheless, the results can be easily extrapolated to a continuous "in-line" configuration, more suitable to industrial purposes.

The Pilot plant

Test-Rig. All the materials used in the test-rig were chosen for their inertness toward organic compounds, in order to prevent any mass loss of aroma compounds by sorption in the test-rig materials. Each liquid was pumped out of its feed reservoir, flowed through the module, and recirculated into the same reservoir (Figure 1). Each circuit was simply composed of a pump and a glass flask (2 L) connected with Teflon tubing (PTFE, Plastibrand, Germany) and all connections were made of stainless steel. The pumps were positive displacement gear pumps with a stainless steel casing and Teflon-coated gears (Micropump U.S.A., model 120 Series). These rotary gear pumps delivered a constant flow rate independent of the downstream pressure of the liquid. Each circuit was also equipped with pressure gauges at the input and the output of the module (Citec, France), (max pressure: 2.5 bars, absolute error: 0.1 bar). The pressure on each side of the membrane was adjusted by means of three stainless steel needle valves (V_2, V_3', V_2', V_3'), (Teesing BV, The Netherlands) and measured with the four pressure gauges. As the speed of the pumps was constant, the flows inside the module were regulated by partly recirculating the fluids to the feed vessels through two bypass valves (V_1 and V_1', Teesing BV, The Netherlands). A cooling bath regulated the temperature of the feeds at 30°C.

Hollow-Fiber Contactor. The experiments were carried out on a microporous hollow fiber membrane module produced by Celgard (Celgard GmbH, Wiesbaden, Germany). This geometry allows a very large contact area with a minimal volume (high compactness). As the membrane material was hydrophobic, the pores were filled with the oil. The module displayed a cross-flow configuration. This was ensured by a baffle located in the middle of the fiber bundle (Figure 2) which compelled the oil to flow from the porous distribution tube (located in the center of the fiber bundle) to the wall of the shell in the first chamber and vice-versa to the collection tube in the second chamber. This was meant to promote turbulence in the fluid flowing outside the fibers, therefore, improving the mass transport through the boundary layer around the fibers. The geometric characteristics of the module are detailed in Table 1. The cumulated volume of the tubing and the fiber-side of the membrane module was equal to 0.5 L, while this volume was equal to 0.25 L for the shell side and the tubing.

We assumed that the mass loss due to flavor sorption on the membrane material was negligible when carrying out oil-water stripping experiments because:

- The calculated permeability (product of the diffusion coefficient and the sorption coefficient) of flavor components in sunflower oil is 10,000 to 100,000 times higher than in polypropylene;
- The contact areas between the aqueous feed phase and the membrane or the oil were similar, and the volume of oil was by far higher than the one of polymer (offering thus a significantly bigger "reservoir" capacity to flavor compounds).

Aqueous Feed Phase. The experiments were done with an aqueous mixture of the aroma compounds listed in Table 2. These 8 compounds have been chosen because they display a wide range of physicochemical properties (hydrophobicity and volatility). The diffusion coefficients of the different solutes have been estimated with the Wilke and Chang method (Reid et al., 1987). We assumed, in our experiments, that the oil/water partition coefficient of each individual aroma compound was not influenced by the presence of the other compounds. Indeed, as the molar fraction of the aroma compounds in the feed or in the stripping phase was very low (in the 10^{-5} to 10^{-7} range), it could be considered that the aroma compounds could not statistically interact with each other (infinite dilution domain).

The concentrations were chosen close to what can be encountered in real food media. Butanal, 2-butanone, 2-hexanone and trans-2-hexenal were the most hydrophilic compounds and were diluted in water with a concentration of 50 PPM (v/v). Ethyl pentanoate, 2-nonanone and ethyl heptanoate, the most lipophilic (that is, oil soluble) molecules, were dissolved in the aqueous phase at 2 PPM (v/v). The concentration of 2-heptanone in the feed was chosen equal to 20 PPM (v/v).

The concentration of the solutes in the stripped phases was measured by static HS-GC. The headspace sample vials were loaded on an automatic sampler (Hewlett Packard 7694 Headspace Sampler) and let equilibrate overnight at 30 °C. The measurement of the composition of the headspace over the samples was performed on a HP 5890 (Hewlett Packard)

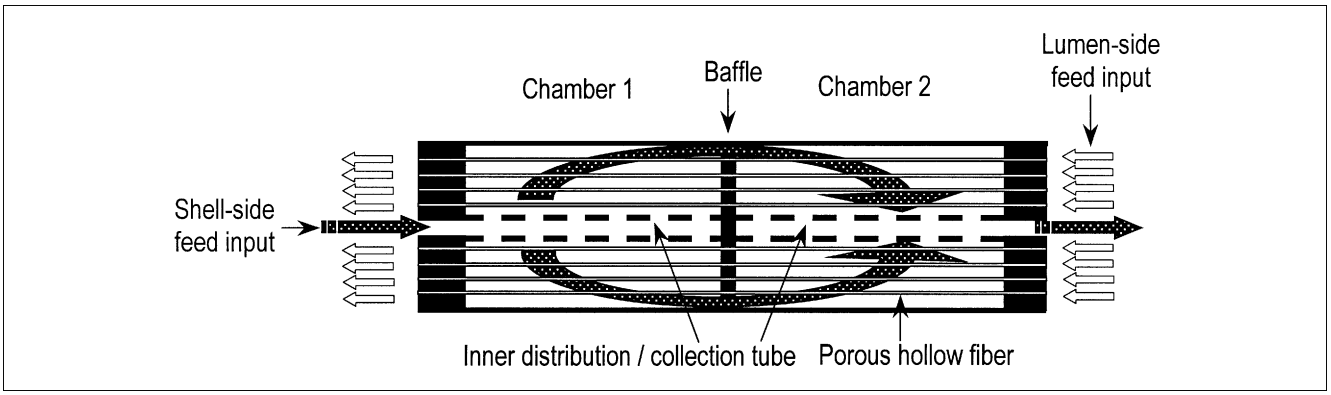

Figure 2. Liquicel Extra-Flow hollow-fiber contactor.

Table 1. Geometric Characteristics of the Tested Hollow Fiber Contactor*

Provider:	Celgard
Contactor type:	Liqui-Cel extra-flow 2.5 in. × 8 in. (64 mm × 203 mm)
Shell diameter	$d_S = 6.3$ cm
Fiber bundle diameter	$d_a = 4.7$ cm
Distribution tube diameter	$d_i = 2.2$ cm
Overall contact area (based on outer fiber diameter)	$A_S = 1.4$ m^2
Overall contact area (based on inner fiber diameter)	$A_F = 1.13$ m^2
Fiber material/type	Polypropylene (X-30)
Number of fibers	9,950
Outer fiber diameter	$d_o = 300$ μm
Inner fiber diameter	$d_F = 240$ μm
Fiber wall thickness	$e = 30$ μm
Fiber porosity	$\epsilon = 0.4$
Pore tortuosity	$\tau = 2.25$
Pore diameter	0.03 μm

*From Schöner et al., 1998.

gas chromatograph equipped with a stainless steel column (30 m × 0.542 mm), packed with DB Carbowax 52 (J&W Scientific, film thickness: 2 μm) and a flame ionization detector (FID). The injector and the detector temperature were respectively maintained at 200 and 250°C. The column was operated from 40 to 225°C with a temperature ramp of 17°C per min. The GC retention times of the studied compound are listed in Table 2. The calibration curves for each compound were linear in the pre-cited range of concentration. As the calibration curves obtained with reference binary solutions (water + each single aroma compound) and with the studied flavor cocktail (water + 8 selected aroma compounds) were similar, it could be concluded that the measured value of the concentration of each compound was not affected by the presence of the other flavor compounds in the sample. The standard deviation was always lower than 4% and the lowest detectable concentration was equal to 0.2 PPM (v/v) for butanal, 0.1 PPM (v/v) for 2-butanone, 2-hexanone and trans-2-hexenal, 0.01 PPM (v/v) for ethyl pentanoate, 2-nonanone and ethyl heptanoate.

Stripping Phase. Commercial sunflower oil (Chempri b.v. Oleochemicals, The Netherlands) was used as the solvent. Its viscosity (42 mPa·s at 30°C) was measured with a CSL^2 Carri-Med rheometer from TA Instruments (Thermal Analysis & Rheology) equipped with a 6 cm diameter cone, 2 deg of angle.

Operating procedures

Starting Procedure. Before each run, a volume of 1.5 L of clean water and 1 L of oil were poured in each feed tank. The liquid which was not wetting the membrane (that is water) first flowed in the module at a flow rate close to 100 L/h. Then, the second pump was started and the oil flow rate was adjusted to the desired value while always keeping the pressure in the aqueous feed higher than in the oil side (at least 0.3 bar transmembrane pressure difference) to prevent any breakthrough of the oil in the aqueous feed. The pressure in the aqueous feed side was regulated by partly closing the valve located at the output of the module (V3 or V3' in Figure 1, depending on the configuration of the experiment). We continuously checked for any cloudiness in the reservoirs or if there was any change in the volumes of the solutions in the feed vessels. Either phenomenon was an indication that one phase was leaking into the other and that an emulsion was forming between the oil and the aqueous solution. If this happened, the experiment had to be aborted and the system cleaned again.

If the two solutions remained clear, the tubing at the output of the module was disconnected from the feed reservoirs and the fluids that flowed through the module (water and oil) were discarded. The water was then replaced in the feed tank by the flavored solution and the aqueous feed flow was adjusted to the desired value. The feed tanks were continuously refilled with the flavored solution and clean oil, in order to keep the liquid level in the reservoirs constant. 2 L of the flavored solution was allowed to flow through to push away the water from the module and the tubing. After that, the tubing at the output of the module was reconnected on the feed reservoirs (which corresponded to the initial time for the experiment). The total aqueous feed phase volume was equal to 1.5 L, while the total sunflower oil volume was equal to 1 L.

Running the Experiments. The kinetic of the extraction was followed for at least 1 h, in order to reach the thermody-

Table 2. Physicochemical Properties of the Tested Aroma Compounds*

Compounds	Structure	Fragrance	$D_W \times 10^{10}$ (m^2·s^{-1})	$D_o \times 10^{10}$ (m·^{2} s^{-1})	BP (°C)	P (Exp)[1]	P (Lit.)	GC Retention Time (min.)
Butanal	C_4H_8O	Pungent	11.1	1.2	74.8	3 ± 0.5	2^{2-3}	3.70
2-butanone	C_4H_8O	Ethereal	11.1	1.2	80	1 ± 0.57	1^{2-3}	4.00
Trans-2-hexenal	$C_6H_{10}O$	Green, fresh	9.2	1	47	17 ± 3	13^{3-4}	10.92
2-Hexanone	$C_6H_{12}O$	Fruity	9.09	0.99	127	14 ± 1	–	7.63
2-Heptanone	$C_7H_{14}O$	Spicy	8.4	0.915	150	54 ± 4	58[5]	9.96
Ethyl pentanoate	$C_7H_{14}O_2$	Apple-like	7.76	0.846	—	170 ± 35	165[4]	8.83
2-Nonanone	$C_9H_{18}O$	Floral, tea	7.36	0.802	194	–	730[6]	14.10
Ethyl heptanoate	$C_9H_{18}O_2$		6.9	0.752	188	–	2000[6]	13.33

P: Partition coefficient between the oil and the aqueous phase: D_w, D_o: Diffusion coefficient, in water and in sunflower oil at 30°C; BP: Boiling Point.
[1]Measured experimentally in the present study at 30°C.
[2]Measured at 25°C (Buttery et al., 1969).
[3]Measured at 25°C (Buttery et al., 1973).
[4]Measured at 25°C (Overbosch et al., 1991).
[5]Measured at 40°C (Druaux, 1997).
[6]Estimated at 30°C with the UNIFAC method (Fredenslund et al., 1975).

namic equilibrium between the two phases. Samples were taken from the aqueous feed vessel every minute during the first 5 min, and then at 10, 30 and 60 min, or more if necessary. The samples were taken from the aqueous feed tank (3 mL) with a glass pipette and poured into 10 mL headspace vials (Hewlett Packard, U.S.A.), which were hermetically sealed with a Teflon septum.

The volume of the samples was small enough to assume that the volume of solution contained by the feed vessel was constant during each experiment.

Cleaning Procedure. At the end of each extraction, while continuously flowing clean water in the aqueous feed side, the oil-filled side of experimental setup was cleaned successively with three organic solvents:

(1) Hexane was applied to permit all the oil to flow away from the shell (as oil oxidation products could foul the pores of the hollow fibers).

(2) Acetone flowed through the module to remove the hexane that could damage the polypropylene fibers.

(3) Pure ethanol was then flown to remove the acetone which could spoil the O-rings in the module.

(4) After having stopped the pumps and emptied the module, dry filtered air was flown in the module to evaporate the remaining traces of ethanol.

Theory

There are two main ways to operate membrane-based solvent extraction with hollow-fiber devices.

- *In Parallel.* The feed and the solvent are flowing in parallel, whether it is cocurrently or countercurrently

- *In Cross Flow.* The fluid in the shell side is then flowing perpendicularly to the fluid flowing in the lumen of the fibers. This configuration is meant to promote turbulence in the shell side, therefore enhancing the mass transfer outside the fibers.

In the first generation of Liqui-Cel modules, the two phases flowed parallel to each other as there was no baffle in the shell. It appeared that channeling could occur in the shell side, especially with low flows, leading to a very poor efficiency for mass transfer in the fluid flowing outside the fibers (Seibert et al., 1993). Since then, Celgard has produced a second generation of Liqui-Cel contactor that contains a baffle at the very center of the fiber bundle in the shell side. Schöner et al., (1998) and Sengupta et al., (1998) have assumed that the flow in the shell side was purely radial and, thus, perpendicular to the fibers (cross-flow configuration). The proposed analytical solutions for the description of the mass balance in the module were very simple, as those authors were working in such conditions that the main resistance to mass transfer was mainly located in the shell.

However, a thorough description of the mass balance in the module when the resistances in the shell and in the lumen side have the same order of magnitude, appears to be more tricky. Seibert and Fair (1997) considered that the Liqui-Cel contactors from the latest generation could be described as a series of two cross-flow extraction steps in series, as they are constituted of two shell side chambers separated by a baffle. For modeling purposes, it was assumed by these authors that both feedstreams were perfectly mixed between the two chambers, although this was not true for the fluid flowing inside the fibers.

Therefore, we decided to rely on an alternative approach to describe the mass transfer inside the transverse flow Liqui-Cel extra-flow module. Indeed, as pointed out by Sengupta et al., (1998), the two phases flowed in a cross-flow pattern in each chamber but on an overall point of view, the feed and the solvent flowed either in cocurrent or in countercurrent patterns. If referring by analogy to heat exchangers, it appears that the equations resulting from parallel flow unbaffled geometries are commonly used to describe the heat balance in more complex configurations, such as baffled shell-and-tube heat exchangers (Jakob, 1957; Kern, 1950). Consequently, we applied this approach to describe the mass transfer in the baffled Liqui-Cel Extra-Flow unit. The relative concentration, that is, the ratio between the concentration at a certain time "t" and the initial concentration of aroma compound in the aqueous feed, is then equal to

$$\frac{C_W(t)}{C_W^0} = \frac{1}{1+V}\left(V + \exp\left(-\frac{1-\exp[-\Phi(1-Q)]}{1-Q\exp[-\Phi(1-Q)]}\right) \times (1+V)\frac{Q_W}{V_W}t\right) \quad (1)$$

with

$$\Phi = \frac{K_{OV}.A_{OV}}{Q_W} = NTU \quad (2)$$

$$Q = \frac{Q_W}{Q_O P} \quad (3)$$

$$V = \frac{V_W}{V_O.P}. \quad (4)$$

'P' is the partition coefficient between sunflower oil and water, which is equal to the flavor compounds concentrations ratio between oil and water at equilibrium. The details of the calculations resulting in Eq. 1 can be found in Dahuron (1987) who worked on counter-flow hollow-fiber contactors.

Results and Discussion

Experimental results

As mentioned earlier, it was chosen to study the effect of the flow of the aqueous feed on the mass transfer between the two phases, as well as the location wherein the fluids were flowing. The sunflower oil flow was always kept constant and equal to 30 L/h. The module was operated with two different configurations:

- *Configuration 1*. The aqueous feed flowed in the shell side while the sunflower oil was flowing inside the lumen of the fibers.

- *Configuration 2*. This configuration constitutes the reverse case to configuration 1: the flavored aqueous feed flowed inside the fibers while the oil was flowing in the shell side.

Nine experiments were carried out with configuration 1, and 12 with configuration 2, varying the aqueous feed flows

from 0.7 L/h to 450 L/h. About 10 samples were taken during each experiment, in order to follow the concentration of the 8 studied aroma compounds in the aqueous feed tank as a function of time. This represents a huge amount of experimental data (more than 1,600) and it would be of little use to display all these results in graphs.

A representative sample of the experimental results is displayed in Figure 3. In this figure the relative concentrations of a homologous series of methyl ketones dissolved in the aqueous feed tank are featured as a function of time.

The following raw conclusions (valid whatever the configuration) can be drawn from the experimental results:

- The relative concentration of the aroma compounds in the aqueous feed tank was first decreasing exponentially, and eventually reached a plateau when the equilibrium between the two phases was reached.
- A higher oil/water partition coefficient led to a faster concentration decrease as a function of time.
- The higher the aqueous feed flow, the faster the mass transfer between the two phases.

The mass-transfer coefficients of the eight aroma compounds were calculated for each experiment, in order to provide a more quantitative and synthetic characterization of the mass transfer between the aqueous feed phase and the sunflower oil.

Evaluation of the Experimental Value of the Overall Mass Transfer Coefficients. Knowing precisely the oil/water partition coefficient P of each aroma compound was a compulsory prerequisite for the calculation of the mass-transfer coefficients. During each experiment, when the equilibrium between the two phases was reached

$$\lim_{t\to\infty}\left(\frac{C_W(t)}{C_W^0}\right)=\frac{V}{1+V} \tag{5}$$

$$\text{and thus, } P=\left[\left\{\left(\lim_{t\to\infty}\left[C_W(t)/C_W^0\right]\right)\right\}^{-1}-1\right]\times\frac{V_W}{V_O} \tag{6}$$

The experimental values of P, obtained from the experimental values of the relative concentration of the aroma compounds in the final plateau stage, were consistent with the values found in the literature (Table 2). This confirmed the assumption that no mass loss of aroma compounds occurred due to sorption in the membrane material, or the module housing. However, when the equilibrium plateau was reached, it was not possible to detect the peaks of 2-nonanone or ethyl heptanoate with the HS-GC apparatus because the concentration in the aqueous feed was lower than the detection threshold of the FID analyzer. Therefore the authors chose to rely on the predicted values listed in Table 2 for the calculation of the mass-transfer coefficients of these two compounds.

The overall mass-transfer coefficient was then deduced from the experimental values of the relative aqueous feed concentration in the exponential decrease zone. Indeed it came easily from Eq. 1

$$K_{OV}=\frac{Q_W}{(1-Q)A_{OV}}\ln\frac{1-\beta Q}{1-\beta} \tag{7}$$

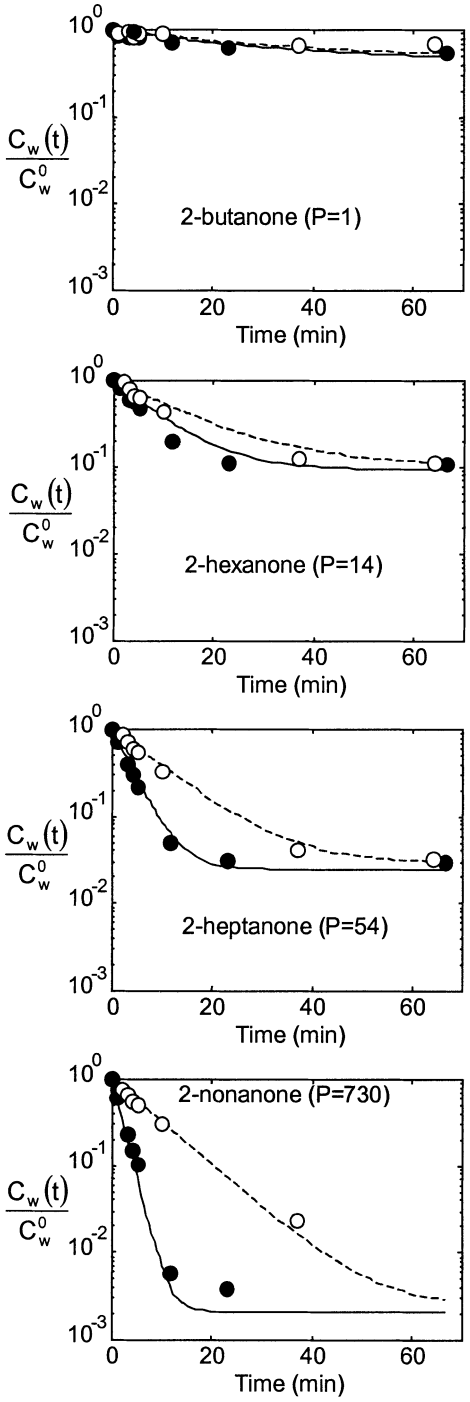

Figure 3. Data sample from stripping experiments: relative concentration of methyl ketones in the aqueous feed vs. stripping time.

Config. 2: constant sunflower oil flow in the shell side = 30 L/h; aqueous feed flow in the lumen side = 12 L/h (----) or 79 L/h (——); temperature = 30°C; overall transfer area = 1.13 m^2.

with

$$\beta=-\ln\left[\frac{C_W(t)}{C_W^0}(1-V)-V\right]\times\left(\frac{V_W}{(1+V)Q_W\times t}\right) \tag{8}$$

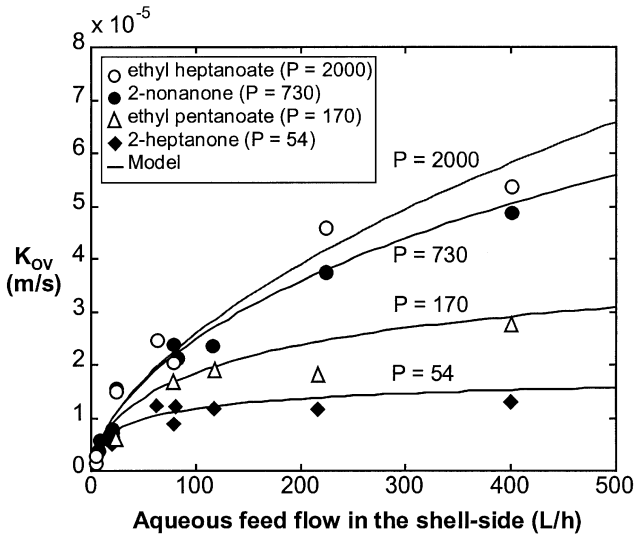

Figure 4. Overall mass-transfer coefficient vs. aqueous feed flow in the shell side.

Config. 1: variable aqueous feed flow in the shell side; constant sunflower oil flow in the lumen side = 30 L/h; temperature = 30°C; overall transfer area = 1.4 m^2.

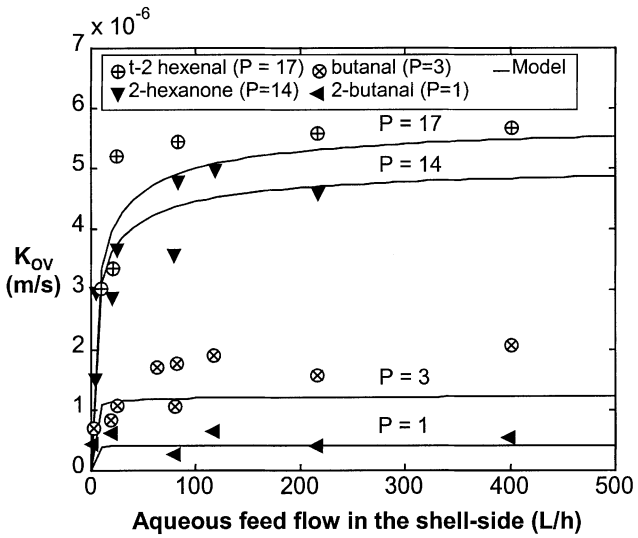

Figure 5. Overall mass-transfer coefficient vs. aqueous feed flow in the shell side.

Config. 1: variable aqueous feed flow in the shell side; constant sunflower oil flow in the lumen side = 30 L/h; temperature = 30°C; overall transfer area = 1.4 m^2.

In our opinion, it is important to point out here that the K_{OV} alone, as a representative indicator of the mass-transfer efficiency, should be used cautiously (whereas this parameter is used as such in most of the articles concerning membrane-based solvent extraction). Indeed, this parameter can be an unexpected source of inconsistency when comparing literature results obtained with different geometries: for instance, whereas most of the authors consider that the area required for the calculation of K_{OV} is the overall membrane area (Gabelman and Hwang, 1999; Prasad and Sirkar, 1992; Malone and Anderson, 1977), others consider that only the effective contact area between the two phases (= overall membrane area $\times$ membrane porosity) is to be taken into account, which would be more consistent with the calculations concerning conventional liquid-liquid contactors (Schöner et al., 1998).

It was chosen to express the overall mass-transfer coefficient as a function of the overall membrane area in this article. Figures 4 and 5 feature the results obtained with configuration 1 ($A_{OV} = 1.4$ m^2, corresponding to the overall membrane area based on the outer diameter of the fibers) while Figures 6 and 7 feature the results obtained with configuration 2 ($A_{OV} = 1.13 m^2$, corresponding to the overall membrane area based on the inner diameter of the fibers).

As a general rule, the higher the oil/water partition coefficient, the higher the value of K_{OV} with fixed operating conditions. In Eq. 7, it appeared that these results were linked to two factors: on the one hand, the slope of the relative concentration of the most lipophilic compounds vs. time was larger than with less lipophilic compounds leading to a higher value of the term $\ln[(1-\beta Q)/(1-\beta)]$ in Eq. 7 and, on the other hand, the value of the stripping factor was higher with the most lipophilic compounds which led to a lowering of Q, and consequently to an increase in the term $Q_W/(1-Q)$ in Eq. 7.

Two distinct trends are shown in Figures 4 to 7.

If the oil/water partition coefficient of the considered aroma compounds was lower than 20, it appeared that the stripping efficiency of both configurations were similar. Moreover, it seemed that the value of the overall mass-transfer area reached a plateau when the aqueous feed flow was higher than 100 L/h.

When the partition coefficient of the aroma compounds was higher than 20, raising the aqueous feed flow led to an

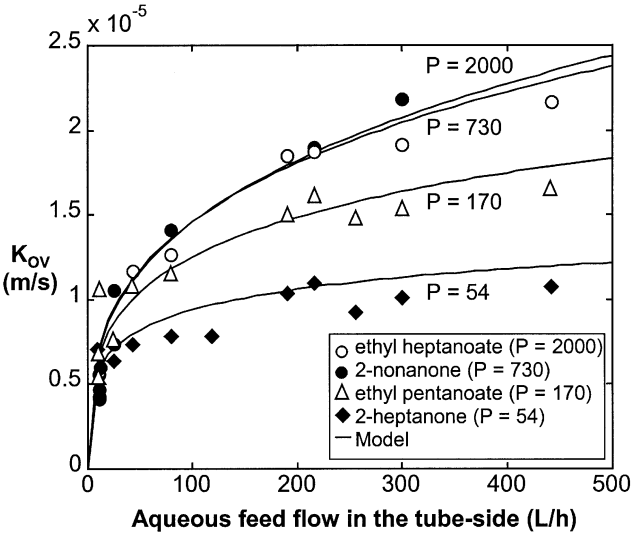

Figure 6. Overall mass-transfer coefficient vs. aqueous feed flow in the tube side.

Config. 2: variable aqueous feed flow in the lumen side; constant sunflower oil flow in the shell side = 30 L/h; temperature = 30°C; overall transfer area = 1.13 m^2.

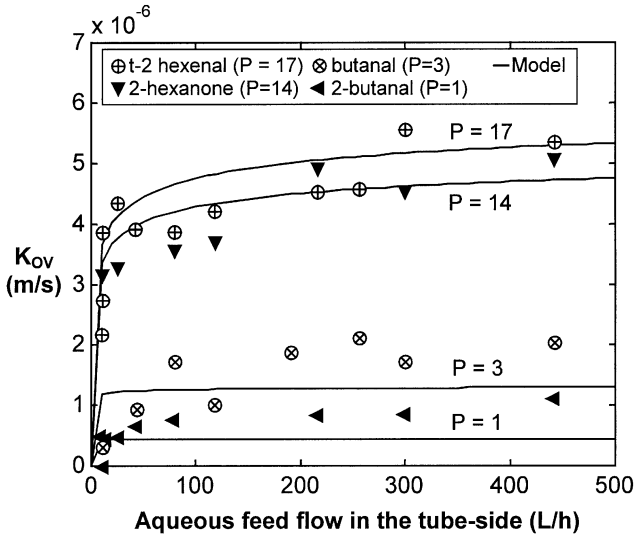

Figure 7. Overall mass-transfer coefficient vs. aqueous feed flow in the tube side.

Config. 2: variable aqueous feed flow in the lumen side; constant sunflower oil flow in the shell side = 30 L/h; temperature = 30°C; overall transfer area = 1.13 m^2.

increase of the overall mass-transfer area, whatever the considered configuration. These results suggest that the main resistance to the mass transport was lying in the boundary layer in the aqueous feed phase.

As a general rule, the stripping is significantly more efficient and faster with the most lipophilic compounds. For instance, the overall mass-transfer coefficient of ethyl heptanoate ($P = 2{,}000$) could reach values more than 100 folds higher than in the case of 2-butanal ($P = 1$) (Figures 4 and 5). This fact illustrated how a MSE operation carried out on an aqueous flavor cocktail with sunflower oil could lead to a selective recovery of the most lipophilic compounds.

Modeling of the mass transport between the two phases

The mass transfer between the flavored water and the sunflower oil can be described with the conventional resistance-in-series approach (Prasad and Sirkar, 1992; Malone and Anderson, 1977). The overall resistance to mass transfer is then equal to the cumulated resistances of the boundary layer in the fluid flowing in the lumen side of the fibers, and the diffusive step through the membrane and the boundary layer in the fluid flowing outside the fibers (in the shell side)

$$\frac{1}{K_{\mathrm{OV}} \cdot A_{\mathrm{OV}}} = \frac{1}{P_{F/W} \cdot K_F \cdot A_F} + \frac{1}{P_{M/W} \cdot K_M \cdot A_{LM}} + \frac{1}{P_{S/W} \cdot K_S \cdot A_S} \tag{9}$$

The explicit values of the parameters used in Eq. 9, and in the forthcoming equations, are detailed in Table 3 as a function of the considered configuration.

Lumen of the Fibers. The flow inside the fibers was always laminar ($Re_F < 2{,}700$). The mass-transfer coefficient characteristic of the boundary layer in the lumen of the cylindrical hollow fibers can then be described with the Lévêque equation (Lévêque, 1928)

Table 3. Different Operating Parameters as Function of the Configuration

Config.	D_F	D_S	η_F	η_S	Q_F	Q_S	$P_{F/W}$	$P_{M/W}$	$P_{S/W}$	A_{OV}
1	D_O	D_W	η_O	η_W	Q_0	Q_W	P	P	1	A_S
2	D_W	D_O	η_W	η_o	Q_W	Q_o	1	P	P	A_F

$$Sh_F = \frac{K_F \cdot d_F}{D_F} = 1.62\left(\frac{d_F}{L} \cdot Re_F \cdot Sc_F\right)^{1/3} \tag{11}$$

with

$$Re_F = \frac{4 \cdot Q_F}{\eta_F \cdot n\pi d_F} \tag{12}$$

and

$$Sc_F = \frac{\eta_F}{D_F}. \tag{13}$$

This correlation was initially a simplified analytical solution of the radial heat transfer within a fluid circulating inside a cylindrical duct with a fully-developed laminar flow. It has been validated experimentally by many authors for mass transfer with hollow-fiber membrane contactors (Urtiaga and Irabien, 1993; Wickramasinghe et al., 1992; Takeuchi et al., 1990; Dahuron and Cussler, 1988; Yang and Cussler, 1986). The Lévêque equation is valid only when the Graetz number characteristic of the fluid flowing inside a duct is higher than 4 (Wickramasinghe et al., 1992), which was always true during our experiments.

Membrane. The transmembrane mass-transfer coefficient is simply a characteristic of a diffusion mechanism through a solvent-filled porous medium

$$K_M = \frac{D_O \cdot \epsilon}{e \cdot \tau}. \tag{14}$$

The geometrical features of the membrane (ϵ,τ,e) have been previously established by Schöner et al., 1998 (Table 1).

Shell side. The mass transfer in the shell side of Liqui-Cel Extra-Flow modules with transverse flow have been previously studied by Schöner et al. (1998). They assimilated the fiber bundle as a densely packed bed and based the mass-transfer correlation on the hydraulic diameter of the bed of fibers and not on the outer diameter of a single fiber, as is conventionally done.

$$Sh_S = \frac{K_S \cdot d_h}{D_S} = \alpha \cdot Re_S^{\beta} \cdot Sc_S^{1/3} \tag{15}$$

with

$$Re_S = \frac{\bar{v}_S \cdot d_h}{\eta_S} \tag{16}$$

$$Sc_S = \frac{\eta_S}{D_S} \tag{17}$$

$$d_h = \frac{d_a^2 - d_i^2 - n d_o^2}{n d_o} \tag{18}$$

$\overline{v_S}$ is the mean radial superficial velocity in the shell side and is obtained by integration

$$\overline{v_s} = \frac{Q_s}{\pi L} \frac{2 \cdot \ln(d_a/d_i)}{d_a - d_i} \tag{19}$$

Schöner et al. (1998) experimentally found that the constant α was equal to 1.76 and that the exponent β over the Reynolds number (related to the mass transfer dependency on the flow in the shell side) was equal to 0.86. The only other modeling results concerning the mass transfer within a fluid flowing in the shell side of baffled Liqui-Cel extra-flow 2.5×8 in. modules were obtained by Sengupta et al. (1998). While carrying out water degasification in the shell side, those authors found that the function *mass transfer vs. flow* was a power law with an exponent β equal to 0.46. The lack of homogeneity concerning those two results led us to experimentally evaluate the resistance to mass transfer in the shell side.

Estimation of the Shell Side Mass Transport. The calculation of the mass-transfer correlation in the shell side was based on the experiments realized with the most lipophilic compounds (ethyl pentanoate, nonanone, and ethyl heptanoate) in configuration 1. Indeed, with those compounds, the boundary layer in the shell side was the main limiting step to mass transfer between the two phases. In other words, the overall mass-transfer coefficient was almost equal in those conditions to the mass-transfer coefficient in the shell side.

The values of the mass-transfer coefficients in the shell were deduced from Eq. 9, combining the calculated values of $K_M \cdot A_{LM}$ and $K_L \cdot A_L$ (Eqs. 11 and 14) with the experimental values of $K_{\mathrm{OV}} \cdot A_{\mathrm{OV}}$

$$K_S \cdot A_S = \left(\frac{1}{K_{\mathrm{OV}}(\exp) A_{\mathrm{OV}}} - \frac{1}{P \cdot K_M \cdot A_{LM}} - \frac{1}{P \cdot K_F \cdot A_F} \right)^{-1} \tag{20}$$

The area A_S of the shell side was based on the overall shell side membrane area ($A_{OV} = 1.4$ m^2). The evolution of the mass-transfer coefficient in the shell side is represented in Figure 8 as a function of the aqueous flow and the Reynolds number in the shell side. The correlation that came out from the experimental results is the following

$$Sh_S = 0.56 Re^{0.62} \cdot Sc^{0.33} \tag{21}$$

The Sherwood dependence on the shell side Reynolds number was found to be very close to other experimental results characteristic of the mass transfer in a fluid flowing perpendicularly to a cylinder ($Sh \propto Re^{0.606}$ (Venkatesh et al., 1994)

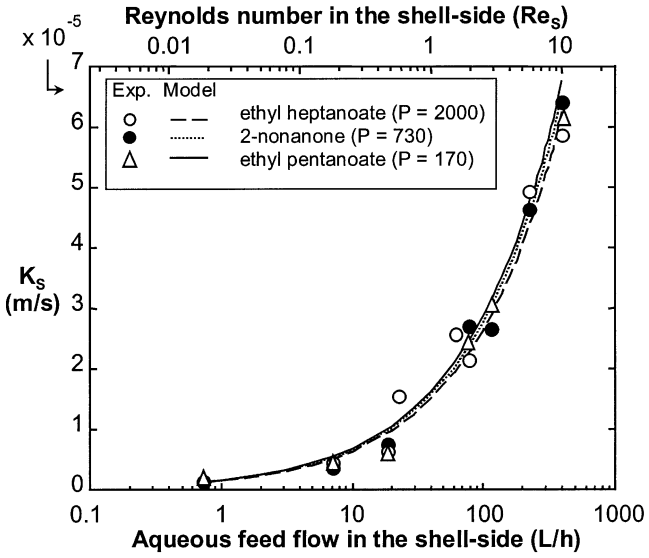

Figure 8. Shell-side mass-transfer coefficient vs. aqueous feed flow and Reynolds number in the shell side.

Config. 1: variable aqueous feed flow in the shell side; constant sunflower oil flow in the lumen side = 30 L/h; temperature = 30 C°; overall transfer area = 1.4 m^2.

or in the shell side of a baffled hollow-fiber contactor ($Sh \propto Re^{0.63}$ (Daiminger, 1996) $Sh \propto Re^{0.6}$ (Imai et al., 1982)). Moreover, by analogy, Eq. 21 follows the same trend as what was observed with baffled shell-and-tube heat exchangers over a wide range of experimental conditions ($Sh \propto Re^{0.6}$ (Donohue, 1949; Short, 1942)).

The literature results concerning the mass transfer in the shell side of the Liqui-Cel extra-flow 2.5 in. ×8 in. (64 mm× 203 mm) module are compared with Eq. 21 in Figure 9. All the results have been expressed with a transfer area equal to the overall shell side membrane area ($A_{OV} = 1.4$ m^2). The equation from Schöner et al. (1998) has been modified from its original form in Figure 9, as those authors chose to express the mass-transfer coefficient in the shell side as a function of the actual contact area between the stripped phase and the solvent ($\epsilon \cdot A_{OV}$), and not the overall membrane area. On the other hand, Sengupta et al. (1998) did not provide any explicit mass-transfer equation in their article. Nevertheless, we expressed the mass-transfer coefficients issued from their experimental results (continuous oxygen removal from water at 20°C in excess sweeping conditions as a function of the water flow in the shell side) in terms of dimensionless numbers ($Sh \cdot Sc^{-1/3}$ *vs.* Re). The physical constants necessary for this calculation (oxygen diffusion coefficient in water, water density and viscosity at 20°C) were found in Janssen and Warmoeskerken (1987). The proposed model (Eq. 21) obtained with ethyl pentanoate, nonanone, and ethyl heptanoate at 30°C is in very good agreement with the experimental values obtained by Sengupta et al. (1998). There is a slight discrepancy between our results and the model from Schöner et al. (1998). This could be attributed to the fact that, in Schöner's configuration, the input of the fluid in the shell side was located at the bottom of the module, whereas, in our setup, it was located at the top of the module. It is

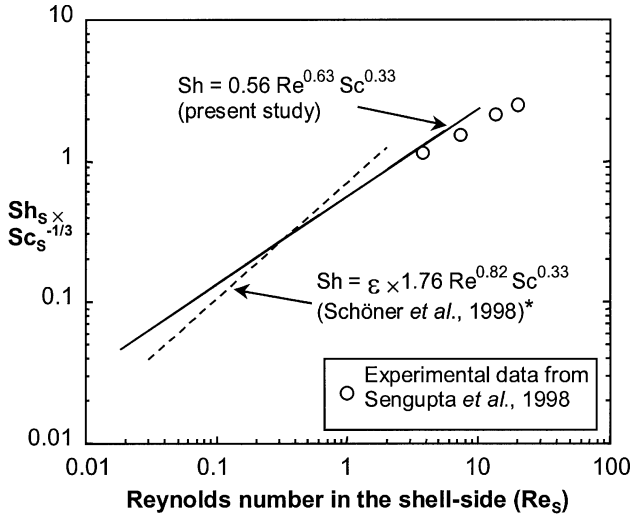

Figure 9. Mass-transfer correlations in the shell side of Celgard Liqui-Cel extra-flow 2.5 in.×8 in. (64 mm×203 mm) contactors.

Overall transfer area = 1.4 m^{2*}. The equation from Schöner et al. (1998) presented in Figure 9 has been modified from its original form to allow a homogeneous comparison with the equation issued from the present work (see in text for more details).

likely that the flow patterns inside the shell could be slightly different in both configurations, especially at lower flows.

Comparison between Model and Experimental Results. The comparison between the calculated values (Eq. 9) and the experimental values of the overall transfer coefficients of each aroma compound is displayed in Figures 4 and 5 for configuration 1 and in Figures 6 and 7 for configuration 2. It appears that the model is in excellent agreement with the experimental data on all the range of operating conditions (aqueous feed flow, configuration), or whatever is the nature of the studied stripped components.

Analysis of the resistance to mass transfer in each configuration

The calculated contribution of each transport step (that is, in the boundary inside the fibers, in the membrane, and in the boundary layer outside the fibers) to the overall mass-transfer resistance is featured as a function of the operating conditions in Figure 10 for configuration 1 and in Figure 11 for configuration 2. These figures point out the limiting steps the limiting steps to mass transfer in both configurations. Each mass-transfer step contribution is represented in Figures 10 and 11 by the combination of its mass-transfer coefficient and its specific exchange area, resulting in the product $K \times A$. Moreover, the oil related transfer steps (represented with dotted lines in Figures 10 and 11) are characterized by the product "$K \cdot A$"×"P" in order to take into account the positive sorption effect of the lipophilic compounds in the sunflower oil. The present representation also allows a consistent comparison of the overall performances of the module in both configurations, thanks to the product '$K_{OV} \times A_{OV}$'.

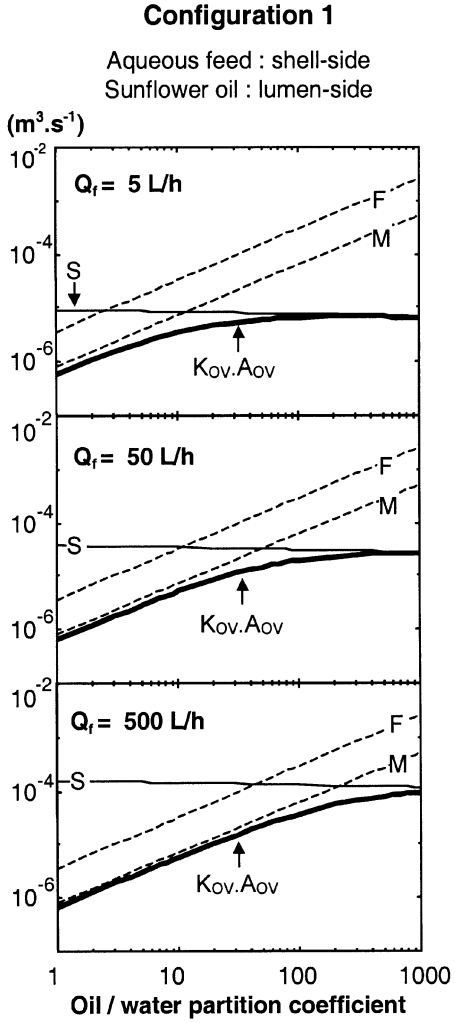

Figure 10. " Apparent" mass-transfer coefficient characteristics of each transfer step.

Boundary layer in the lumen side of the hollow fibers [F], membrane [M], boundary layer in the shell side [S] as a function of the operating conditions. Sunflower oil flow = 30 L/h; temperature = 30°C;–transport step through the aqueous phase;---- transport step through Sunflower oil. Configuration 1: $S = K_S \cdot A_S$; $F = P \times K_F \cdot A_F$; $M = P \times K_M \cdot A_M$.

In order to complete Figures 10 and 11, it was necessary to express the diffusion coefficients of the extracted compounds as a function of the oil/water partition coefficient. Therefore, we estimated the values of the diffusion coefficients of aldehydes, methyl ketones, and ethyl esters ranging from C4 to C9 with the Wilke-Chang method and expressed them as a function of their respective oil/water partition coefficients. We obtained the following relationships, valid only for the aforementioned compounds, with a regression coefficient of more than 99.9%

$$D_W = 1.1 \times 10^{-9} - 5.8 \times 10^{-11} \ln(P) \quad (22)$$

$$D_o = 1.2 \times 10^{-10} - 6.1 \times 10^{-12} \ln(P). \quad (23)$$

The following trends could be deduced from Figures 10 and 11.

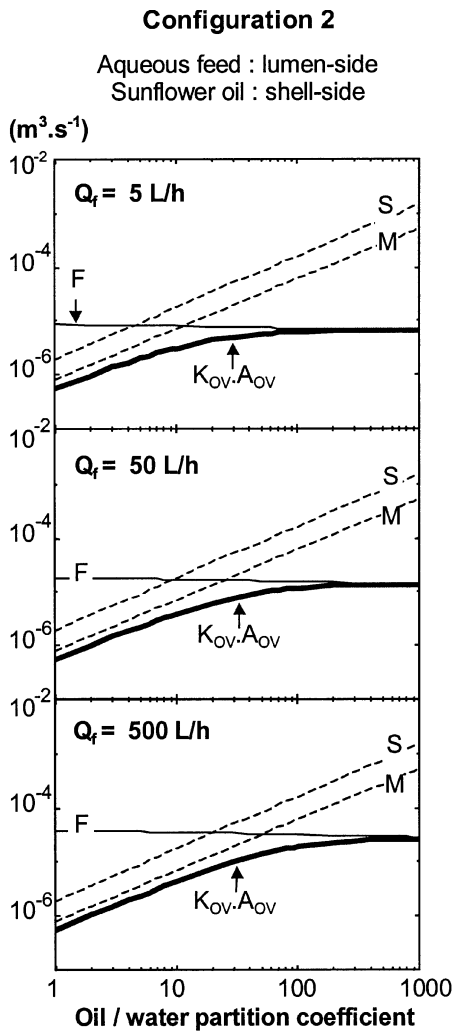

Figure 11. " Apparent" mass-transfer coefficient characteristics of each transfer step.

Boundary layer in the lumen side of the hollow fibers [F], membrane [M], boundary layer in the shell side [S] as a function of the operating conditions. Sunflower oil flow = 30 L/h; temperature = 30°C; —transport step through the aqueous phase; ---- transport step through sunflower oil. Configuration 2: $S = P \times K_S \cdot A_S$; $F = K_F \cdot A_F$; $M = P \times K_M \cdot A_M$.

The main resistance to the mass transfer of the least lipophilic compounds ($P < 20$) was located in the sunflower oil, whatever the considered configuration. This was due to the very low value of the diffusivity of the aroma compounds in the oil if referring to water ($D_O \approx D_W/10$). Moreover, it appeared that the main resistance to the mass transport for the least lipophilic compounds ($P < 20$) was always located in the oil-filled membrane, whatever the configuration or the operating conditions (with an oil flow equal to 30 L/h).

With higher oil/water partition coefficients, the effect of the preferential sorption of the lipophilic compounds in the oil was prevailing over their low diffusivity, leading to an increase of their apparent mass-transfer coefficients in the oil as a function of the oil/water partition coefficient.

Consequently, the resistances of the oil-filled transport steps gradually became negligible in comparison with the resistance in the aqueous phase. For very high oil/water partition coefficients ($P > 100$), the overall mass-transfer coefficient tended to equal the mass transfer in the aqueous phase. As a consequence, raising the aqueous feed flow resulted in an increase of the overall mass-transfer coefficient. However, the apparent mass-transfer coefficient in the water was slightly diminishing with an increasing oil/water partition coefficient. As aforementioned, this was due to the fact that, with the studied compounds, an increase in oil/water partition coefficient was synonymous to an increase in molecular weight, resulting in a slight diffusivity decrease.

If comparing the overall transfer coefficients for aqueous feed flows higher or equal to 50 L/h, it is noticeable that configuration 1 was more efficient than configuration 2 for the stripping of the most lipophilic compounds.

Figures 12 and 13 show a synthetic representation of the overall performances of the Liqui-Cel Extra-Flow 2.5 in.×8 in. (64 mm×203 mm) module in both configurations as a function of the operating conditions. These figures are meant to provide the reader with an easy-to-use tool allowing a synthetic estimation of the performances the Liqui-Cel extra-flow 2.5 in.×8 in. (64 mm×203 mm) module. In these figures, the volumetric mass-transfer coefficient ($K_{OV} \cdot a$) isovalue curves are featured as a function of the aqueous feed flow and the oil/water partition coefficient. "a" is the specific interfacial area as defined by Treyball (1963), that is, the overall contact area per unit equipment volume ($a = A_{OV}/V_S$). As it was previously shown that the oil flow was not significantly influencing the overall mass transfer, we believe that those curves are also valid whatever the sunflower oil flow, provided it is higher than 30 L/h.

Two specific zones were distinguished in Figure 12, representing the performances of configuration 1:

- Zone A (in the upper left corner), characteristic of the compounds with a low P. In this area, most of the resistance (more than 80%) to mass transfer is located in the membrane. Consequently, the aqueous feed flow does not have any influence on the mass transfer, which explains the vertical orientation of the $K_{OV} \cdot a$ isovalue curves in the upper lefthand corner of Figure 12. Moreover, it seems that the membrane tends to act as a barrier, with regard to the very low values of the mass-transfer coefficients ($K_{OV} \cdot a < 10^{-2}$ s^{-1}).

- Zone B (in the lower righthand corner), characteristic of the compounds with a high P. Contrary to the former case, most of the resistance is only located in the aqueous phase. Therefore, this explains the fact that an increase of the aqueous flow leads to a very significant increase of mass-transfer coefficient.

These remarks allow us to state again that MSE operated with high aqueous feed flows, can prove to be a selective extraction tool. Indeed, with aqueous feed flows higher than 100 L/h, the extraction performance is very high for the very lipophilic compounds (Zone B) whereas the oil-filled membrane acts, as a barrier for the least lipophilic compounds (Zone A). This is a rather unusual way to use the MSE technique, as it is commonly admitted that the membrane only acts as an immobilizer for the interface between the two contacting liquids, and should offer the least resistance to mass transfer. However, operating MSE, in such a way could be

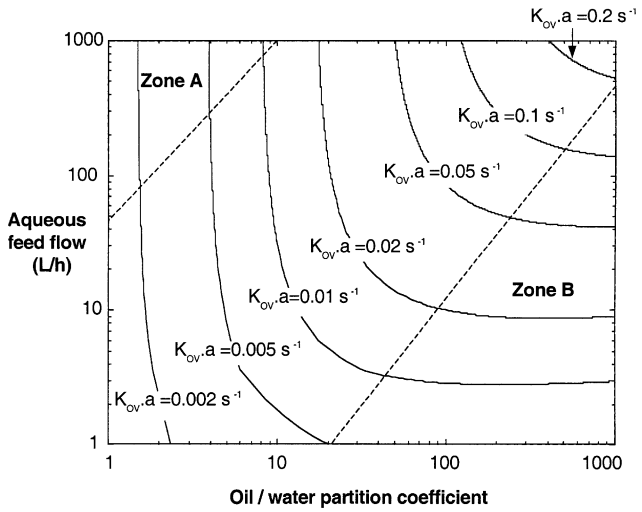

Figure 12. Configuration 1: overall volumetric mass-transfer coefficient as a function of operating conditions (Zone A: more than 80% of the overall resistance to mass transfer is located in the membrane; Zone B : more than 80% of the overall resistance to mass transfer is located in the shell-side).

Constant sunflower oil flow in the lumen side = 30 L/h; Variable aqueous feed flow in the shell side; temperature = 30°C; overall transfer area = 1.4 m^2; specific interfacial area 'a' = 3,000 m^{-1}.

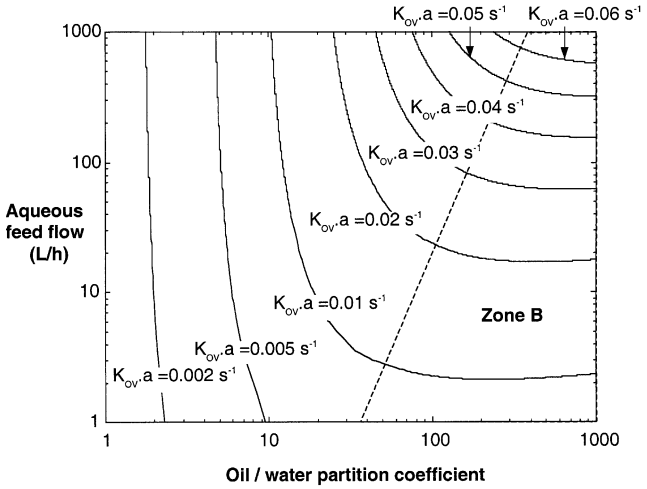

Figure 13. Configuration 2: overall volumetric mass-transfer coefficient as a function of operating conditions (Zone B: more than 80% of the overall resistance to mass transfer is located in the tube side).

Constant sunflower oil flow in the shell side = 30 L/h; variable aqueous feed flow in the lumen side; temperature = 30°C; overall transfer area = 1.13 m^2; specific interfacial area 'a' = 2,400 m^{-1}.

very convenient if a fractionation based on the lipophilicity of the aroma compounds is to be achieved.

Figure 13 shows the same type of overall mass transfer isovalue curves characteristic of configuration 2. The same trends as in Figure 12 can be observed, but the values of the mass-transfer coefficients for the most lipophilic are significantly lower with configuration 2 than with configuration 1. Consequently, the segregating performances between very lipophilic compounds and the least lipophilic compounds are lower. Nevertheless, it is important to point out here that, from a more practical point of view, configuration 2 should sometimes still be preferred, because it is much easier to clean the lumen of the fibers than the outer part of the fiber bundle, especially if the aqueous feed is very viscous or contains particles in suspension (like living cells).

MSE applied to the flavor field : advantages and perspectives

It appears clearly in Table 4 that MSE offers significantly higher stripping performances than the other conventional liquid-liquid extraction devices. However, whether MSE offers better performances than columns because of an enhanced mass transfer or because of the high specific interfacial area of hollow fiber bundles, it is not clear. Indeed, whereas those two parameters can be clearly identified with MSE, it is always hard to dissociate the respective effects of the mass-transfer coefficient and the specific interfacial area in the "$K_{OV}\cdot a$" product with contacting columns. Nevertheless, the hollow fiber modules are generally designed to offer the largest interfacial area possible, which constitutes their main technological advantage. As an illustration, the specific interfacial area of a rotating column has been roughly estimated by Kiani et al. (1984) as close to 200 m^{-1}, whereas a value of 3000 m^{-1} was obtained with the Liqui-Cel extra-flow 2.5 in.$\times$ 8 in. (64 mm$\times$203 mm) module operated in configuration 1.

Concerning the food/biological industry field more specifically, the other main advantage of MSE comes from its nondispersive nature. Indeed, when operating conventional contacting devices, the desemulsification of the aqueous feed and solvent would be particularly tricky, as food/biological liquids contain most of the time surface-active components, like proteins, polysaccharides, or emulsifying additives.

The MSE technique proves to be a selective separation technique as it offers high transport rates through the membrane for the flavor compounds displaying a high affinity for the solvent, while the membrane merely acts as a barrier for the compounds with a low affinity for the solvent. Therefore, varying the nature of the solvent and/or the operating conditions will allow the monitoring of the flavor composition of the aqueous stream at the output of the membrane contactor. This principle was used by Ho and Sheridan (1998) who managed to extract the heavier flavor compounds from beer with the MSE technique, while keeping ethanol and lighter compounds in the feedstream. The model proposed in the present article, could constitute a very valuable and innovative formulation tool for food technologists willing to monitor the sensory profile of foodstreams, although this model was developed primarily to optimize a separation operation. In the authors' opinion, this application of MSE shows how chemical engineering tools could help to design products with consumer-attractive functionalities, illustrating in the process the present trend that drives chemical engineering tech-

Table 4. Performance of Several Solvent Extraction Devices

Extractor Type	$K_{ov} \cdot a \times 10^4$ (s^{-1})	L (m)	V (cm^3)	Ref.
Rotating column	7	2×1	630	Ding and Cussler (1992)
Conventional column	0.5	2×14	9,000	Ding and Cussler (1992)
Hollow fibers	530	2×0.32	8	Ding and Cussler (1992)
Hollow fibers	656—131	—	—	Kiani et al. (1984)
Hollow fibers*	2,000—20	0.15	470	present work
Hollow fibers**	600—10	0.15	470	present work

*Celgard Liqui-Cel Extra-Flow 2.5 in. × 8 in. contactor, config. 1.
**Celgard Liqui-Cel Extra-Flow 2.5 in. × 8 in. contactor, config. 2.

niques from "process engineering" to "product engineering" (Cussler, 2000; Wintermantel, 1999).

Conclusions

The extraction of aroma compounds from aqueous model solutions to sunflower oil through a commercial baffled hollow fiber contactor was carried out over a wide range of operating conditions. The influence of the location where the stripped feed was flowing (the lumen side of the fibers or the shell side) was studied. It was shown that the boundary layer in the aqueous feed was the limiting step for the mass transfer of the most lipophilic compounds. With similar operating conditions, the mass transfer was more efficient in the shell side than in the lumen side. On the other hand, the oil-filled membrane merely acted as a barrier for the least lipophilic compounds. Eventually, two synthetic graphs representing the overall stripping performances of the Liqui-Cel extra-flow 2.5 in. ×8 in. (6.4 mm×203 mm) module as a function of the operating conditions, as well as the affinity of the flavor compound to be extracted, were proposed. These tools are intended to help the food technologists or the flavor experts willing to monitor the sensory profile of a flavor cocktail obtained with the MSE technique described in the present article.

Acknowledgments

The authors express their sincere thanks to Dr. J. Schneider (Celgard GmbH, D-65174 Wiesbaden, Germany) and J. Munoz (Celgard, 13800 South Lake Drive, Charlotte, NC 28273) for their advice and fruitful comments, as well as to Prof. Dr. W. G. M. Agterof, Dr. ir. G. E. J. Vaessen and ing. J. W. M. Seijen ten Hoorn from the food processing group, URV, for their support all along this study. We would also like to thank warmly ing. L. van Pierik and ing. D. Taal, from the Flavour Unit of URV, for having kindly handled the GC analysis of our numerous samples.

Notation

a = specific interfacial area, m^{-1}
A_F = inner area of the hollow fibers, m^2
A_{LM} = logarithmic mean area of the membrane, m^2
A_{OV} = contact area between the two phases, m^2
A_S = oil/water contact area outside the hollow fibers, m^2
BP = boiling point, °C
$C_w(t)$ = concentration of aroma compounds in the aqueous feed at time t, kg/m^3
C^0 = initial concentration in the aqueous feed, kg/m^3
D = diffusion coefficient of the aroma compounds, m^2/s
d_a = diameter of the fiber bundle, m
d_i = diameter of the distribution/collection tube in the Liqui-Cel extra-flow contactor, m
d_F = inner diameter of the hollow fibers, m
d_h = hydraulic diameter of shell, m
d_o = outer diameter of the hollow fibers, m
d_S = diameter of the shell chamber, m
e = thickness of the fibers, m
$HS\text{-}GC$ = gas chromatography coupled to a headspace sampling
K = mass-transfer coefficient, m/s
K_{OV} = overall mass transfer coefficient, m/s
L = length of the hollow fibers, m
MSE = membrane-based solvent extraction
n = number of hollow fibers in the contactor
$P_{F/W}$ = partition coefficient between the fluid flowing in the lumen-side of the hollow fibers and water, dimensionless
$P_{M/W}$ = partition coefficient between the fluid filling the pores of the membrane and water, dimensionless
P = oil/water partition coefficient, dimensionless
$P_{S/W}$ = partition coefficient between the fluid flowing in the shell side and water, dimensionless
Q = capacity factor, dimensionless
Q_F = flow inside the hollow fibers, m^3/s
Q_O = sunflower oil feed, flow, m^3/s
Q_S = flow in the shell side, m^3/s
Q_W = aqueous feed flow, m^3/s
Re = Reynolds number, dimensionless
Sc = Schmidt number, dimensionless
Sh = Sherwood number, dimensionless
t = time, s
v = velocity, m/s
V = volume factor, dimensionless
V_O = sunflower oil volume, m^3
V_S = volume of the empty shell, m^3
V_W = aqueous feed volume, m^3

Greek letters

α = constant in Eq.15, dimensionless
β = constant in Eq. 15, dimensionless
ϵ = porosity of the membrane, dimensionless
η = kinematic viscosity, m^2/s
τ = tortuosity of the membrane, dimensionless
Φ = number of transfer units, NTU

Subscripts

F = fluid flowing in lumenside of the fibers
h = hydraulic diameter of the fiber bundle
M = membrane
O = sunflower oil
S = fluid flowing in the shell side
W = aqueous feed phase

Literature Cited

Baudot, A., and M. Marin, "Pervaporation of Aroma Compounds: Comparison of Membrane Performances with Vapour-Liquid Equilibrium and Engineering Aspects of Process Improvement," *Trans. IChemE (Food Bioprod. Process.)*, **75**, 117 (1997).

Buttery, R. G., L. C. Ling, and D. G. Guadagni, "Flavor Compounds: Volatilities in Vegetable Oil and Oil-Water Mixtures. Estimation of Odor Thresolds," *J. Agric. Food Chem.*, **21**, 198 (1973).

Buttery, R. G., L. C. Ling, and D. G. Guadagni, "Volatilities of

Aldehydes, Ketones, and Esters in Dilute Water Solution," *J. Agric. Food Chem.*, **17**, 385 (1969).
Cussler, E.L. "Will Changes in the Chemical Industry Spark Changes in this Journal?," *Chem. Eng. Sci.*, **55**, 1039 (2000).
Dahuron, L., and E. L. Cussler, "Protein Extraction with Hollow Fibers," *AIChE J.*, **34**, 383 (1988).
Dahuron, L., "Designing Liquid-Liquid Extraction in Hollow Fiber Modules," PhD Diss., Univ. of Minnesota, Minneapolis (1987).
Daiminger, U. "Reactive Extraction in Hollow Fiber Modules: Advantages and Limits of a New Separation Technique," PhD Diss., Technical University of Munich, Munich, Germany (1996).
Ding, H. B., and E. L. Cussler, "Racemic Leucine Separation by Hollow-Fiber Extraction," *AIChE J.*, **38**, 1493 (1992).
Donohue, D. A., "Heat Transfer and Pressure Drop in Heat Exchangers," *Ind. Eng. Chem.* **41**, 2499 (1949).
Druaux, C., "Influence of the Physico-Chemical Characteristics of a Molten Cheese on its Texture and its Flavour," PhD Diss., University of Burgundy, Dijon, France (1997).
Fabre, C. E., P. J. Blanc, A. Marty, G. Goma, I. Souchon, and A. Voilley, "Extraction of 2-Phenylethyl Alcohol by Techniques Such as Adsorption, Inclusion, Supercritical CO_2, Liquid-Liquid and Membrane Separations," *Perfumer & Flavourist*, **21**, 27 (1996).
Frank, G. T., and K. K. Sirkar, "Alcohol Production by Yeast Fermentation and Membrane Extraction," *Biotech. Bioeng. Symp. Ser.*, **15**, 621 (1985).
Fredenslund, A., R. Jones, and J. M. Prausnitz, "Group-Contribution Estimation of Activity Coefficients in Nonideal Liquid Mixtures," *AIChE J.*, **21**, 1086 (1975).
Gabelman, A., and S. T. Hwang, "Hollow Fiber Membrane Contactors," *J. Memb. Sci.*, **159**, 61 (1999).
Ho, S. V., and P. Sheridan, "A Membrane Process for Making Enhanced Flavor Fluids," *Int. Patent*, **WO 99/33949** (1998).
Imai, M., S. Furusaki, and T. Miyauchi, "Separation of Volatile Materials by Gas Membranes," *Ind. Eng. Chem. Des. Dev.*, **21**, 421 (1982).
Jakob, M., *Heat Transfer,* Vol. 2, Wiley, New York (1957).
Janssen, L. P. B. M., and M. M. C. G. Warmoeskerken, *Transport Phenomena Data Companion,* A. Arnold Ltd, London (1987).
Kern, D. Q., *Process Heat Tranfer,* Mc Graw-Hill, New York (1950).
Kiani, A., R. R. Bhave, and K. K. Sirkar, "Solvent Extraction with Immobilized Interface in a Microporous Hydrophobic Membrane," *J. Memb. Sci.*, **20**, 125 (1984).
Lévêque, M.A., "Les Lois de la Transmission de Chaleur par Convection," *Ann. Mines*, **13**, 201 (1928).
Malone, D. M., and J. L. Anderson, "Diffusional Boundary-Layer Resistance for Membranes with Low Porosity," *AIChE J.*, **23**, 177 (1977).
Overbosch, B, W. G. M. Agterof, and L. C. Ling, "Flavor Release in the Mouth," *Food Rev. Int.*, **7**, 137 (1991).
Prasad, R., and K. K. Sirkar, "Membrane-Based Solvent Extraction" in W. S. W. Ho, and K. K. Sirkar, eds., *Membrane Handbook,* Van Nostrand Reinhold, New York, **727** (1992).
Prasad, R., and K. K. Sirkar, "Solvent Extraction with Hydrophilic and Composite Membranes," *AIChE J.*, **33**, 1057 (1987).
Reid, R. C., J. M. Prausnitz, and H. E. Poling, *Properties of Gases and Liquids*, McGraw-Hill, New York (1987).
Schöner, P., P. Plucinski, W. Nitsch, and U. Daiminger, "Mass Transfer in the Shell Side of Cross Flow Hollow Fiber Modules," *Chem. Eng. Sci.*, **53**, 2319 (1998).
Seibert, A. F. and J. R. Fair, "Scale-Up of Hollow Fiber Extractors," *Sep. Sci. Technol.*, **32**, 573 (1997).
Seibert, A. F., X. Py, M. Mshewa, and J. R. Fair, "Hydraulics and Mass Transfer Efficiency of a Commercial-Scale Membrane Extractor," *Sep. Sci. Technol.*, **28**, 343 (1993).
Sengupta, A., P. A. Peterson, B. D. Miller, J. Schneider, and C. W. Fulk, "Large-Scale Application of Membrane Contactors for Gas Transfer from or to Ultrapure Water," *Sep. Purif. Technol.*, **14**, 189 (1998).
Short, B. E., "A Review of Heat-Transfer Coefficients and Friction Factors for Tubular Heat Exchangers," *Trans. ASME*, **64**, 779 (1942).
Souchon, I., J. A. Rojas, A. Voilley, and G. Grevillot, "Trapping of Aromatic Compounds by Adsorption on Hydrophobic Sorbents," *Sep. Sci. Technol.*, **31**, 2473 (1996).
Souchon, I., "Continuous Extraction of Lactones Produced by Microbiological Means," PhD Diss., University of Burgundy, Dijon, France (1994).
Spinnler, H. E., L. Dufossé, I. Souchon, A. Latrasse, C. Piffaut-Juffard, A. Voilley, and P. Delest, "Production of Gamma-Decalactone Using Bioconversion," French Patent No. **FR 93/06673** (1994).
Starmans, D. A. J., and H. H. Nijhuis, "Extraction of Secondary Metabolites from Plant Material: A Review," *Trends Food Sci. Technol.*, **7**, 191 (1996).
Takeushi, H., K. Takahashi, and M. Nakano, "Mass Transfer in Single Oil-Containing Microporous Fiber Contactors," *Ind. Eng. Chem. Res.*, **29**, 1471 (1990).
Treybal, R. E., *Liquid Extraction,* 2nd ed., Mc Graw-Hill, New York (1963).
Urtiaga, A. M., and J. A. Irabien, "Internal Mass Transfer in Hollow Fiber Supported Liquid Membrane," *AIChE J.*, **39**, 521 (1993).
Venkatesh, M., K. A. Narayan, and R. P. Chabra, "An Experimental Study of Mass Transfer from a Sparingly Soluble Cylinder in Cross Flow Configuration," *Chem. Eng. Comm.*, **130**, 181 (1994).
Wickramasinghe, S. R., M. J. Semmens, and E. R. Cussler, "Mass Transfer in Various Hollow Fiber Geometries," *J. Memb. Sci.*, **69**, 235 (1992).
Wintermantel, K., "Process and Product Engineering: Achievements, Present and Future Challenges," *Trans. IChemE*, **77**, 175 (1999).
Yang, M. C., and E. L. Cussler, "Designing Hollow-Fiber Contactors," *AIChE J.*, **32**, 1910 (1986).

Manuscript received June 20, 2000, and revision received Jan. 4, 2001.